Fuel Processing Technology 228 (2022) 107137

Contents lists available at ScienceDirect

Fuel Processing Technology

journal homepage: www.elsevier.com/locate/fuproc

Optimization of multiple-stage fuel injection and optical analysis of the combustion process in a heavy-duty diesel engine

Minhoo Choi, Sungwook Park *

School of Mechanical Engineering, Hanyang University, 222 Wangsimni-ro, Seongdong-gu, Seoul 04763, Republic of Korea

ARTICLE INFO

Keywords:
Multiple injections
Pilot injection
Post injection
Particulate matter
Endoscopic visualization

ABSTRACT

The goals of this study were to optimize multiple-stage fuel injections and optically analyze the effects of multiple injections of fuel on the combustion process in a heavy-duty compressed ignition engine. The engine experiments consisted of pilot injection and post-injection experiments. The pilot injection quantities and timings were varied. The post-injection quantities and number of post injections were analyzed. Combustion images was obtained to calculate the flame temperature and soot density. The results revealed that premixed combustion by a single injection led to engine noise and vibration because of the long ignition delay. The optimal pilot injection strategy improved the engine noise, vibration, thermal efficiency, and nitrogen oxide emissions. However, a pilot injection induced diffusion combustion, and an increase in particulate matter emissions was inevitable. The optimized post-injection promoted the oxidization of incomplete combustion materials and provided a lower peak cylinder pressure, resulting in low nitrogen oxides and particulate matter emissions. The combustion images revealed that the pilot injection caused a moderate increase in flame temperature and high soot production. The post injection, however, effectively reduced the soot density during the late combustion period, resulting in a low soot density at the end of the observation period.

1. Introduction

Compressed ignition (CI) engines have been widely used in various industries because of their high efficiency, which is attributed to their high compression ratio, low pumping loss, and lean air-fuel mixture conditions [1,2]. In particular, the tremendous power of heavy-duty CI engines has been used in transportation, construction, and power plants, making human life more comfortable and convenient. However, large amounts of emission gases are attributed to CI engines, and air pollution has become a global issue. Nitrogen oxides (NOx) and particulate matter (PM) emitted from CI engines cause environmental problems and have harmful effects on human health [3–6]. To solve these emissions problems, emissions regulations have been tightened in the USA, Europe, and Asia over the past decade [7]. In addition, various studies have been conducted by engine researchers to implement premixed combustion in CI engines. As a result, low-temperature combustion techniques, such as early injection, homogeneous charge compression ignition (HCCI), premixed charge compression ignition (PCCI), and reactivity-controlled compression ignition (RCCI) strategies, have been developed to provide meaningful reductions in NOx and PM emissions [8–14]. However, these combustion techniques have several limitations. Because a considerable amount of power is required in various industries using heavy-duty CI engines, low-temperature combustion has limited application in these industries and is accompanied by a high fuel consumption [9–14]. Owing to the CI engine characteristics, premixed combustion causes knocking combustion, which is accompanied by engine noise and vibration, deteriorating engine durability and power [9]. Moreover, unburned gases, such as total hydrocarbon (THC) and carbon monoxide (CO), can increase because of the lean equivalence ratio and low combustion temperature [9,10]. For these reasons, conventional combustion techniques and diesel fuel have been widely used in heavy-duty CI engines, and various studies have attempted to not only improve the

Abbreviations: ACHR, Accumulated heat release; aSOE, After start of energizing; aTDC, After top dead center; bTDC, Before top dead center; CA, Crank angle; CCD, Charge coupled device; CFD, Computational fluid dynamics; CI, Compressed ignition; CO, Carbon monoxide; CO_2, Carbon dioxide; DPF, Diesel particulate filter; EGR, Exhaust gas recirculation; FSN, Filter smoke number; HCCI, Homogeneous charge compression ignition; NOx, Nitrogen oxides; O_2, Oxygen; PCCI, Premixed charge compression ignition; PM, Particulate matter; RCCI, Reactivity controlled compression ignition; ROHR, Rate of heat release; SCR, Selective catalyst reduction; TDC, Top dead center; THC, Total hydrocarbon.

* Corresponding author at: School of Mechanical Engineering, Hanyang University, 222 Wangsimni-ro, Seongdong-gu, Seoul 04763, Republic of Korea.
E-mail address: parks@hanyang.ac.kr (S. Park).

https://doi.org/10.1016/j.fuproc.2021.107137
Received 9 September 2021; Received in revised form 19 November 2021; Accepted 12 December 2021
Available online 17 December 2021

engine efficiency and combustion stability but also reduce their NOx and PM emissions by applying multi-injection strategies along with the installation of after-treatment systems such as selective catalyst reduction (SCR) and diesel particulate filters (DPFs) [15–18]. Multiple-injection strategies are divided into pilot injection and post injection, depending on the injection timing. The purposes of the pilot and post injections are different.

The pilot injection strategy involves the injection of a small amount of diesel fuel before the main fuel injection, which increases the combustion chamber temperature. As a result, engine noise and vibration are reduced during the main combustion period by reducing the ignition delay. Previous studies have shown that a pilot injection greatly reduces engine noise and vibration [17–20]. An investigation of the effect of a pilot injection on engine performance in an optical engine was carried out by Tanaka et al. [17]. They found that reductions in combustion noise and emissions were possible by minimizing the pilot injection quantity and advancing the pilot injection timing. However, it was revealed that excessive reduction and advancement of the pilot injection parameters can deteriorate engine performance. In addition to engine noise and vibration, the fuel consumption was improved by the pilot injection [18,21]. Although a pilot injection promotes diffusion combustion, which is attributed to NOx formation, an optimized pilot injection has been reported to decrease NOx emissions [20,22–26]. However, various studies have reported different PM emission trends. Some studies have confirmed that a pilot injection adversely affects PM emissions [19,20,24–27]. In contrast, some investigations have indicated that a pilot injection reduces PM emissions [22,28,29]. A previous study conducted by Ishida et al. [26] focused on the effects of pilot injection quantity and timing on combustion and emission characteristics in a turbo-charged, direct-injection diesel engine. Their study reported that delaying pilot injection significantly reduced flame temperature and NOx emissions. However, higher smoke emissions were observed under pilot injection conditions. They recommended a small pilot injection quantity to reduce NOx emissions and fuel consumption.

Whereas the main goal of a pilot injection is to reduce engine noise and vibration, the purpose of a post injection is to oxidize incomplete combustion products. After the main injection, the post-injection strategy promotes oxygen (O_2) utilization by enhancing air-fuel mixing in the combustion chamber. Previous studies reported that a post injection was very effective in reducing PM and unburned gas emissions [30–35]. Hotta et al. [30] explored the effects of a post injection on engine performance using an optical engine and 3D-CFD analysis. The combustion images and CFD results obtained by them revealed that the jet flame formed by a post injection carried the remaining soot in the squish area. As both the temperature and O_2 utilization increased, soot could be oxidized. Various studies on post-injection quantities and timings have been performed to improve the effects of post injections. Farhan et al. [34] conducted experiments to analyze the combustion and emission characteristics of CI engines with different post-injection timings and quantities. They demonstrated that a post injection effectively reduces HC emissions under 40% and 60% engine operating loads, and it is important to optimize the post-injection quantity and timing to reduce NOx and PM emissions. Other studies have reported that suitable post-injection timing is an important factor for oxidation [35–37]. However, poor results for emissions and fuel consumption have been reported under inappropriate post-injection conditions. The increase in dwell time between the main and post injections resulted in higher PM emissions and fuel consumption [31,38].

Although conventional engine experiments have been conducted, it is impossible to perform an optical analysis of the combustion phenomenon occurring in the combustion chamber; moreover, indirect analysis methods only provide limited information. Optical engine experiments have been performed to support the analysis of experimental results to overcome the limitations of conventional engine experiments. In particular, as optical equipment devices have been developed, an endoscope system that can preserve the combustion chamber geometry was applied to enhance engine research. In addition, advanced combustion image processing technology helps to measure the flame temperature and soot density through combustion images [39]. Various engine studies have been conducted by combining an endoscope system and combustion image processing technology [40,41]. Cheng et al. [40] investigated the effects of multiple-injection parameters on the combustion and soot characteristics of a heavy-duty diesel engine. Combustion images demonstrated that increasing the pilot injection quantity and advancing the pilot injection timing decreased soot formation, but increased the flame temperature, which led to high NOx emissions. Iorio et al. [41] compared diesel combustion and methane and diesel dual-fuel combustion in terms of the flame temperature and soot density. According to their study, the flame temperature and soot density of dual-fuel combustion were lower than those of diesel combustion, regardless of the experimental conditions, resulting in low NOx and PM emissions under dual-fuel combustion conditions.

Although numerous studies have been performed to overcome the disadvantages of diesel engines, few studies have focused on a comprehensive analysis of multiple-stage injection strategies. Furthermore, the lack of detailed quantitative optical research makes it difficult to identify the effect of multiple-stage injection on the combustion process. The main objectives of this study were to optimize multiple-stage injections and perform an optical analysis of the effects of multiple injections on the combustion process in a heavy-duty diesel engine. This study reveals that an optimized multiple-injection strategy can improve the combustion and exhaust characteristics of CI engines. Furthermore, it reveals the effects of pilot and post injections on flame temperature and soot density through combustion image analysis.

2. Experimental method

2.1. Experimental apparatus

A single-cylinder, heavy-duty CI engine was used to carry out the experiments. The specifications of the engine are listed in Table 1. A schematic of the engine setup is shown in Figs. 1(a) and 1(b). In the present study, there were a number of equipment groups for each objective. Fig. 1(a) illustrates the equipment groups used in the engine experiments. The single-cylinder, heavy-duty CI engine was operated using a 55 kW DC motor at a constant speed. The mass flow controller, surge chamber, and heater were included in the intake system, and this system supplied the intake mixture under constant volume and temperature conditions. In this study, diesel was used as the main fuel for the engine experiments, and the fuel injection quantity, pressure, and timing were controlled by the common rail and NI-CompactRIO system. The HORIBA emission bench and AVL smoke meter were connected to the exhaust port, and the emission materials were measured. In the emission bench, NOx, THC, and CO were detected, and the emissions were recorded in ppm. The smoke meter only measured the PM, which was converted into units of filter smoke number (FSN). In addition, lambda values were acquired using the lambda sensor, which was connected to the exhaust port. An NI-DAQ board was used to acquire and save the experimental results. For each experimental condition, 100 cycles of data were acquired, and the average and standard deviation values were calculated. Different engine heads were used, depending on

Table 1
Engine specifications.

Item	Description
Compression Ratio	17.0
Bore (mm)	107
Stroke (mm)	126
Connecting Rod (mm)	200
Displacement Volume	1100
Nozzle Hole Number	9
Nozzle Hole Diameter (mm)	0.161

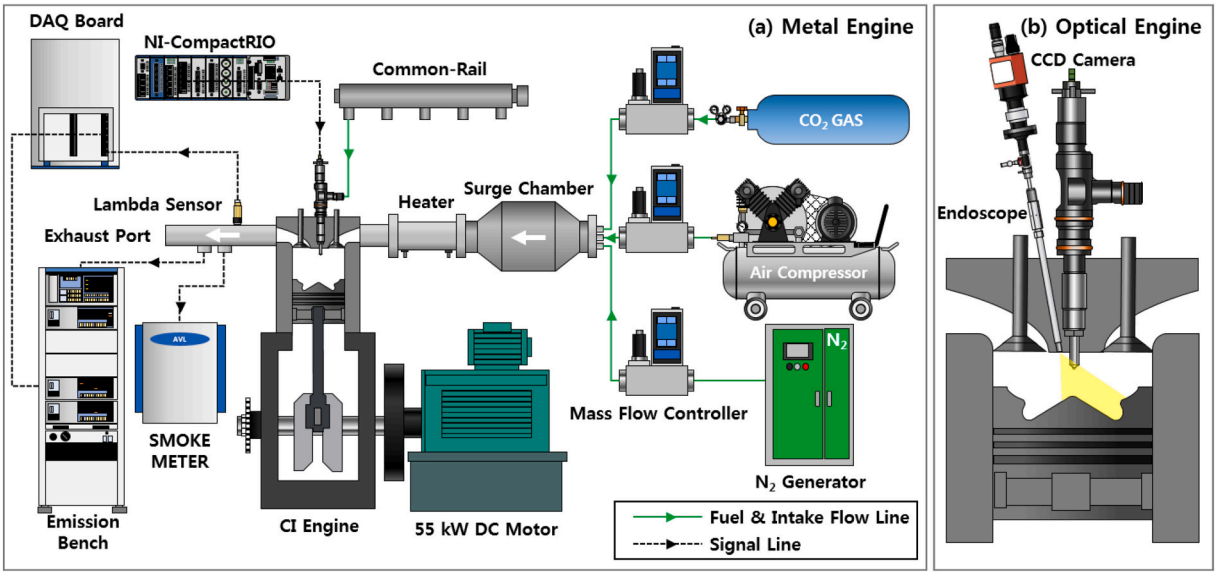

Fig. 1. Schematic of the (a) metal engine and (b) optical engine setup.

the objective of the experiments, whereas the other equipment remained unchanged. One of the engine heads was used for the conventional experiments, and the other engine head was modified for optical combustion experiments and equipped with an endoscope system. Fig. 1(b) shows the setup of the optical engine. The endoscope penetrated the engine head and was inserted into the combustion chamber. A 30° endoscope was selected to simultaneously observe the combustion chamber and the tip of the nozzle. A lightweight charge-coupled device (CCD) camera was installed at the end of the endoscope to prevent damage to the endoscope due to engine vibration during the combustion experiment. The camera trigger was created using NI-CompactRIO and was delayed by the camera software program. To reduce experimental variation, at least 10 combustion images were acquired and averaged for each experimental case.

2.2. Experimental conditions

The engine experiments were performed in accordance with the specified operating conditions by controlling the experimental devices. The reference experimental conditions are summarized in Table 2. The reference conditions were maintained in all experiments. In particular, the total fuel injection quantity was fixed at 51 mm^3/cycle. To analyze the effects of multiple injections, various values for the injection timing and quantity and number of injections were utilized in this study. The multiple injections consisted of a pilot, main, and post injection in that order. The main injection timing was fixed at 0.13° after top dead center (aTDC) regardless of the experimental conditions. The pilot injection occurred before the main injection, and the post injection was performed after the end of the main injection. The multiple injection experiments were divided into pilot injection and post-injection experiments. It was possible that multiple pilot injections would negatively affect engine performance by increasing noise, vibration, and fuel consumption, and increase engine emissions, such as NOx emissions. Therefore, in this study, a single pilot injection was utilized in the experiments. Details of the pilot injection conditions are listed in Table 3. The pilot injection quantities were varied from 3 to 9 mm^3/cycle with a 3 mm^3/cycle interval, and the pilot injection timing was varied from aTDC −5.7° to −12.5° at crank angle (CA) intervals of 3.4°. The main fuel injection quantity was reduced by the pilot injection quantity to ensure that the total fuel injection quantity for each experiment was the same. If the pilot or post injection quantity were reduced below 3 mm^3/cycle, which is lower than 5.88% of the total fuel injection quantity, incomplete combustion would occur, and the multi-stage injection would have negative effects on engine performances. Therefore, this study determined the fuel injection quantity of 3 mm^3/cycle as the standard unit for multiple injections.

After the pilot injection experiments, post-injection experiments were performed. To analyze only the effects of the post injection on combustion and emission characteristics, the pilot injection parameters and main injection timing were maintained in all cases. Because the total fuel injection quantity was fixed, the main injection quantity was determined by the sum of the pilot and post-injection amounts. The post-injection experiments were divided into single and multiple post-injection experiments, depending on the number of post injections. Detailed experimental conditions are listed in Table 4. Generally, the post injection was conducted during the expansion stroke. If the post-injection timing is retarded from the TDC, the cylinder temperature is reduced, making it difficult for the injected fuel to completely combust. As a result, the unburned gases and PM emissions increase, and the engine efficiency deteriorates. Therefore, it was more effective to ensure that the post-injection timing was close to the main injection timing. The single-stage post-injection experiments were focused only on post-injection quantities. The timing of the single-stage post injection was fixed at aTDC 9.2°, and the post-injection quantity was varied from 3 to 9 mm^3/cycle with a 3 mm^3/cycle interval. Two- and three-stage post

Table 2
Reference experimental conditions.

Item	Description
Engine Speed (RPM)	1250
Oil & Coolant Temperature (°C)	80
Intake Temperature (°C)	40
Intake Pressure (bar)	1.4
EGR Rate (%)	20
Fuel Injection Pressure (bar)	1020
Total Fuel Injection Quantity (mm^3/cycle)	51

Table 3
Experimental conditions for pilot injection.

Item	Description
Pilot Injection Quantity (mm^3/stroke)	3, 6, 9
Pilot Injection Timing (deg, aTDC)	−5.7, −9.1, −12.5
Main Injection Quantity (mm^3/stroke)	51 – Pilot Injection Quantity
Main Injection Timing (deg, aTDC)	0.13

Table 4
Experimental conditions for post injection.

Item	Description	
Pilot Injection Quantity (mm^3/stroke)	3	
Pilot Injection Timing (deg, aTDC)	−5.7	
Main Injection Quantity (mm^3/stroke)	51 – Pilot & Post Injection Quantity	
Main Injection Timing (deg, aTDC)	0.13	
Post Injection Quantity (mm^3/stroke)	Single-Stage	3, 6, 9
	Multiple-Stage	6 + 3, 9 + 3, 6 + 6, 6 + 6 + 6
Post Injection Timing (deg, aTDC)	9.2, 14.0, 18.8	

injections were carried out during the multiple-stage post-injection experiments. The multiple-injection timing was selected from aTDC 9.2° to 18.8° at intervals of 4.8° CA. The pilot injection was a single injection condition, whereas the post injection consisted of multiple injections. To prevent interference between multiple injected fuels due to a short interval, the interval of post injection was 1.4° CA longer than that of the pilot injection. The combustion images were acquired at intervals of 3° CA from the fuel injection timing.

2.3. Methodology for analysis

2.3.1. Ringing intensity theory

Multiple injections helped to prevent engine noise and vibrations. To confirm these effects, it is necessary to quantify engine noise and vibration. For this reason, the ringing intensity theory has been widely used by researchers [42,43]. The ringing intensity represents the knocking combustion, and it is expressed as follows:

$$Ringing\ Intensity = \frac{1}{2\gamma}\frac{\left(\beta\frac{dp}{dt_{max}}\right)^2}{P_{max}}\sqrt{\gamma RT_{max}} \tag{1}$$

In this equation, β is a constant value of 0.05, and γ represents the specific heat ratio [43]. In this study, ringing intensity was calculated during the post-processing of the experimental data using the NI LabView program. The ringing intensities were compared with respect to the variety of multiple injection conditions.

2.3.2. Combustion image processing theory

Combustion images were acquired during the optical experiments. However, a simple analysis of images does not yield meaningful results. Therefore, the present study applied the combustion image processing theory to calculate the flame temperature and soot density from the combustion images. To apply this theory, the luminance of soot from two lights with different wavelengths was measured. The flame temperature and soot density can be calculated based on the apparatus temperature [39,40,44,45]. The combustion image processing equation can be expressed as follows:

$$e^{\frac{C_2}{\lambda T_a}} = \left(1 - e^{-\frac{KL}{\lambda^\alpha}}\right)e^{-\frac{C_2}{\lambda T}} \tag{2}$$

where T and T_a are the true and apparatus temperatures, respectively. KL represents the soot density, which is the product of the absorption coefficient that is proportional to the soot density and flame thickness. In the visible range, the constant value α is equal to 1.38. C_2 is the second radiation constant in Planck's law [45]. Eq. (2) can be expressed as

$$KL = -\lambda_1^\alpha ln\left[1 - e^{\left(-\frac{C_2}{\lambda_1}\left(\frac{1}{T_{a1}}-\frac{1}{T}\right)\right)}\right] \tag{3}$$

$$KL = -\lambda_2^\alpha ln\left[1 - e^{\left(-\frac{C_2}{\lambda_2}\left(\frac{1}{T_{a2}}-\frac{1}{T}\right)\right)}\right] \tag{4}$$

The true flame temperature and soot density can be obtained by solving the nonlinear polynomial eqs. (3) and (4) at different wavelengths. KL is a dimensionless value and is affected by image acquisition conditions such as the exposure time of the camera, brightness coefficient, and lens angle. If the image acquisition conditions are different, even if the acquired KL values are the same, the same soot density is not indicated. Therefore, although the KL value derived from the flame image cannot be analyzed as a quantitative value, it can help researchers to understand the qualitative trend of soot density according to changes in experimental conditions.

Prior to performing the optical experiments and obtaining the combustion images, calibration of the apparent temperature using a standard light source is essential. Among the light sources, a black body provides the most accurate values because it has the highest emissivity, and the error of the apparent temperature can be minimized [45,46]. In addition to the black body, a tungsten lamp was used for calibration to analyze the combustion image [39]. Because the tungsten lamp has a gray body, which has a lower emissivity than the black body, an error of approximately 200 K in flame temperature can occur. Despite the above error, it was considered that meaningful results could be derived from the combustion images.

Therefore, in this study, tungsten lamps (apparent temperature of 2850 K) were used for calibration. Because the endoscope was equipped with a blue light filter, red and green colors were selected among the three colors. The wavelengths showing the maximum absorption rates of the red and green colors in the CCD camera were 620 nm and 540 nm, respectively, and the apparent temperatures at 620 nm and 540 nm were calculated, respectively. Approximate values of the flame temperature and soot density were calculated using MATLAB. The flame temperature and soot density obtained from the original images are shown in Fig. 2.

3. Results and discussion

3.1. Pilot injection experiments

The engine experiments were performed for various pilot injection quantities and injection timings. Fig. 3 presents the results of cylinder pressure and rate of heat release (ROHR) with respect to the CA under various pilot injection quantities and injection timing conditions. The results clearly reveal that the effects of the pilot injection on combustion are different in case of single or multiple injections. The single-injection case showed a large increase in ROHR. In contrast, the experimental results of pilot injection showed a lower gradient of ROHR than that of a single injection during main combustion, regardless of the pilot injection quantity and injection timing. The difference in the combustion characteristics is closely related to the multiple-injection strategy. In a single injection, the ROHR was divided into two regions, that is, premixed combustion and diffusion combustion regions, because of the increased ignition delay. Without the pilot injection, the cylinder temperature was not sufficient to ignite the injected fuel in the combustion chamber, which increased the ignition delay and resulted in the formation of a homogeneous air-fuel mixture. In the early combustion stage, premixed combustion rapidly occurred with a homogeneous air-fuel mixture, which can cause knocking combustion. Therefore, in the CI engine using diesel fuel, a high compression ratio was applied to prevent knocking combustion. Subsequently, the injected fuel was ignited quickly, resulting in moderate diffusion combustion in the late combustion stage. Even though diesel combustion occurred, premixed combustion accounted for a significant portion of diesel combustion under single-injection conditions, and the highest value of ROHR was observed during premixed combustion. In contrast, a low intensity of premixed

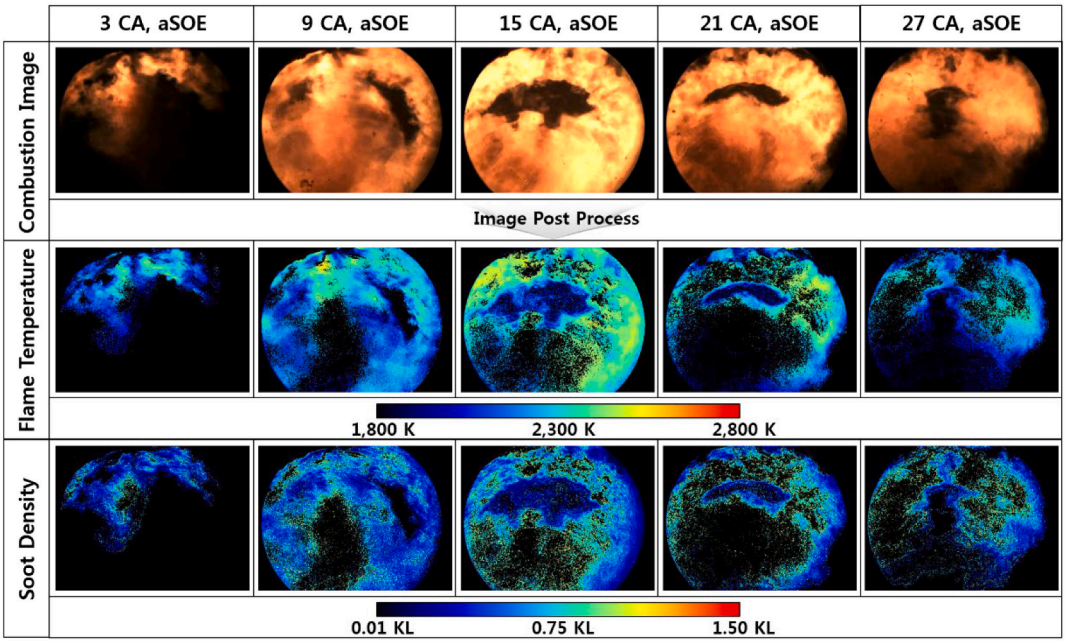

Fig. 2. Flame temperature and soot density calculated from the combustion images.

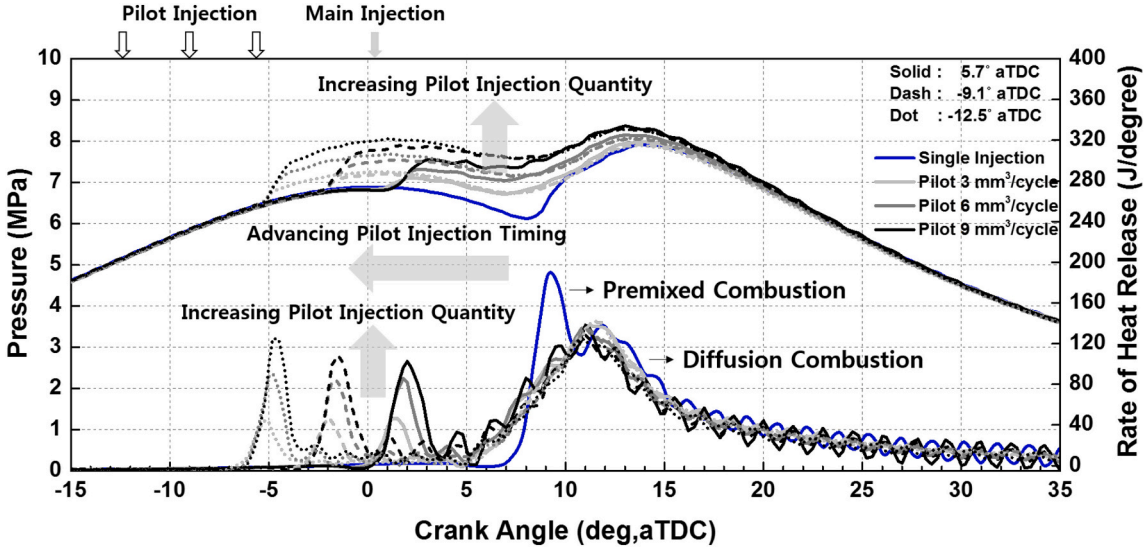

Fig. 3. Effects of pilot injection strategies on cylinder pressure and ROHR.

combustion occurred when a pilot injection preceded the main injection. This resulted in an increased cylinder temperature during the main injection. As a result, significant reductions in the ignition delay and peak value of the ROHR were observed. Diffusion combustion is dominantly observed regardless of the pilot injection timing and quantity. In the multiple-injection cases, higher pilot injection quantities resulted in higher peak cylinder pressures. Moreover, as the pilot injection timing advanced, the timing of the increase in cylinder pressure also advanced. The main purpose of the pilot injection is to prevent the occurrence of knocking rather than to improve thermal efficiency or reduce NOx and PM emissions.

Fig. 4 shows the effects of pilot injection quantities and timings on ringing intensity. The ringing intensity, which quantitatively represents the knocking combustion intensity, is related to the noise and vibration of the engine. A higher ringing intensity indicates that a higher engine noise and vibration has occurred. Under single-injection conditions, high-intensity premixed combustion occurred, resulting in the highest ringing intensity. The pilot injection decreased the ringing intensity. This figure demonstrates that the pilot injection effectively prevents engine noise and vibration by suppressing premixed combustion. However, increasing the pilot injection quantity and advancing the pilot injection timing increased the ringing intensity, causing engine noise and vibration. As a result, a large pilot injection quantity and an excessively high advanced injection timing had negative effects on engine combustion. In.

particular, increasing the pilot injection quantity resulted in a higher ratio of premixed combustion. The ringing intensity was higher than that of a single injection with the largest and most advanced pilot injection conditions, indicating that the engine noise and vibration were more severe. The effects of the pilot injection were confirmed by the engine performance. Figs. 5(a) and 5(b), respectively, provide the indicated mean effective pressure net (IMEPnet) and thermal efficiency

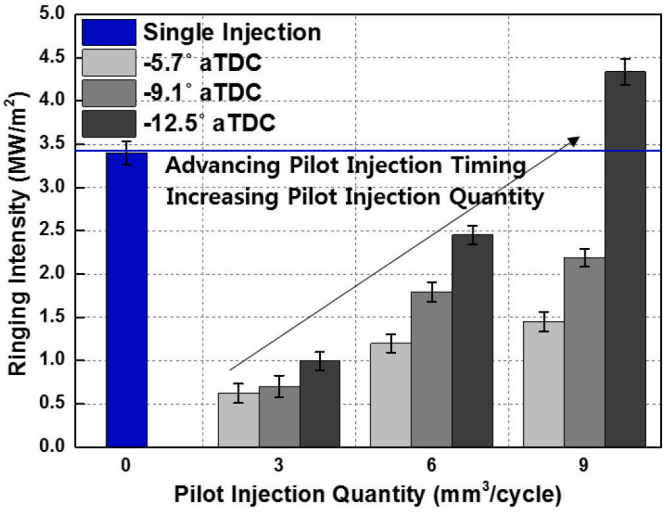

Fig. 4. Effects of pilot injection strategies on ringing intensity.

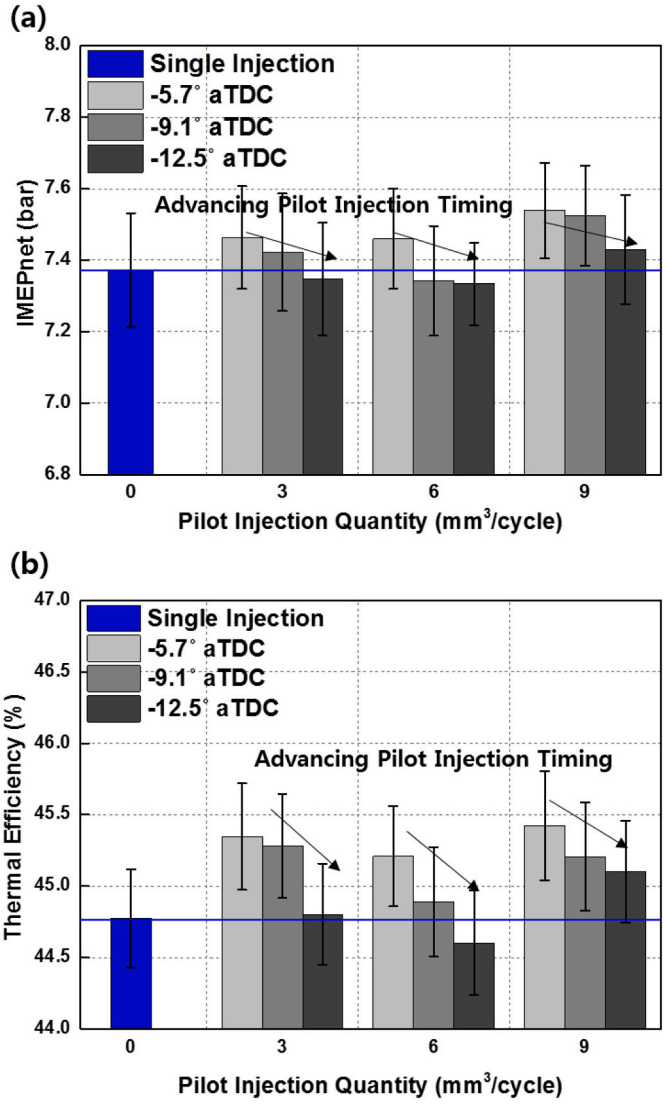

Fig. 5. Effects of pilot injection strategies on (a) IMEPnet and (b) thermal efficiency.

for various pilot injection strategies. As shown in the figure, unlike those obtained under the single-injection conditions, the engine performances for various pilot injection parameters were located in the error range. Nevertheless, the effects of the pilot injection on the engine performance could be clearly observed. Regardless of the pilot injection quantity, a better performance was achieved at a pilot injection timing of aTDC –5.7° than with a single injection. However, it was found that advancing the pilot injection timing deteriorated both the IMEPnet and thermal efficiency simultaneously. This is closely related to the effect of the pilot injection on combustion phasing. The short ignition delay caused by applying the pilot injection rapidly increased the cylinder pressure. While the cylinder pressure after TDC resulted in positive work, the increased cylinder pressure before TDC caused negative work. For the cases where the pilot injection timing was closest to the main injection timing, the cylinder pressure was increased after TDC, as illustrated in Fig. 3. However, the cylinder pressure increased before TDC because the pilot injection timing was advanced from the main injection timing, impairing the IMEPnet and thermal efficiency of the engine. Furthermore, a high cylinder pressure results in heat loss, which adversely affects the engine efficiency. In addition to the IMEPnet and thermal efficiency, the NOx and PM emissions were affected.

by the pilot injection. Fig. 6(a) shows the effects of the pilot injection parameters on the NOx emissions and peak cylinder pressure, demonstrating that the NOx emissions were mainly affected by the pilot injection quantity. According to previous research, NOx emissions are closely related to the combustion temperature [9]. Therefore, a

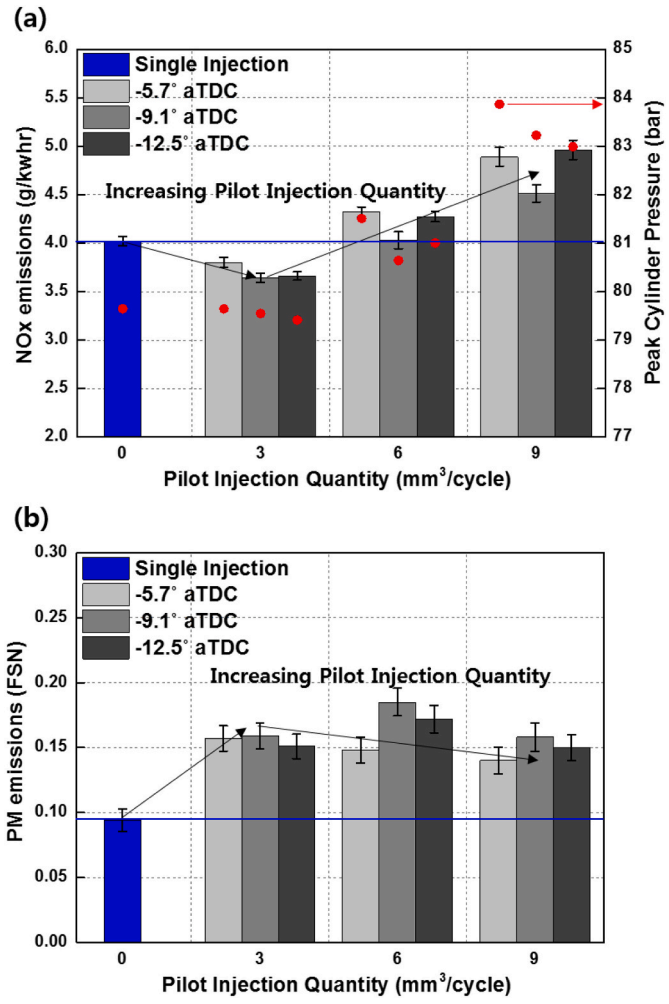

Fig. 6. Effects of the pilot injection on (a) NOx emissions, peak cylinder pressure, and (b) PM emissions.

proportional relationship between the NOx emissions and peak cylinder pressure can be observed in this figure. Under the conditions of a pilot injection quantity of 3 mm^3/cycle, both the NOx emissions and peak cylinder pressure were lower than those under the single-injection condition because the premixed combustion, which rapidly increases the cylinder pressure, is prevented by the pilot injection. However, as the pilot injection quantity increased further, the NOx emissions and peak cylinder pressure steadily increased. This figure demonstrates that NOx formation is effectively suppressed by reducing the peak cylinder pressure only for a pilot injection quantity of 3 mm^3/cycle. Fig. 6(b) shows that the PM emissions of the pilot injection cases were always higher than those of the single-injection case. Because of the long ignition delay with a single injection, a homogeneous air-fuel mixture was formed, resulting in a higher ratio of premixed combustion. In contrast, the ignition delay was shortened by the pilot injection, and a locally rich air-fuel mixture was formed. Soot typically forms at low temperatures and when mixtures with high equivalence ratios are heated, and it comprises materials such as sulfur, water, and hydrocarbons. Therefore, it is inevitable that PM emissions will be increased by applying a pilot injection.

For the pilot injection cases, the higher the pilot injection quantity, the lower the PM emissions, and this is a trade-off relationship with both the NOx emissions and peak cylinder pressure. The above results reveal that the NOx and PM emissions were more affected by the pilot injection quantity than by the pilot injection timing. In summary, the experimental results revealed that a pilot injection quantity of 3 mm^3/cycle

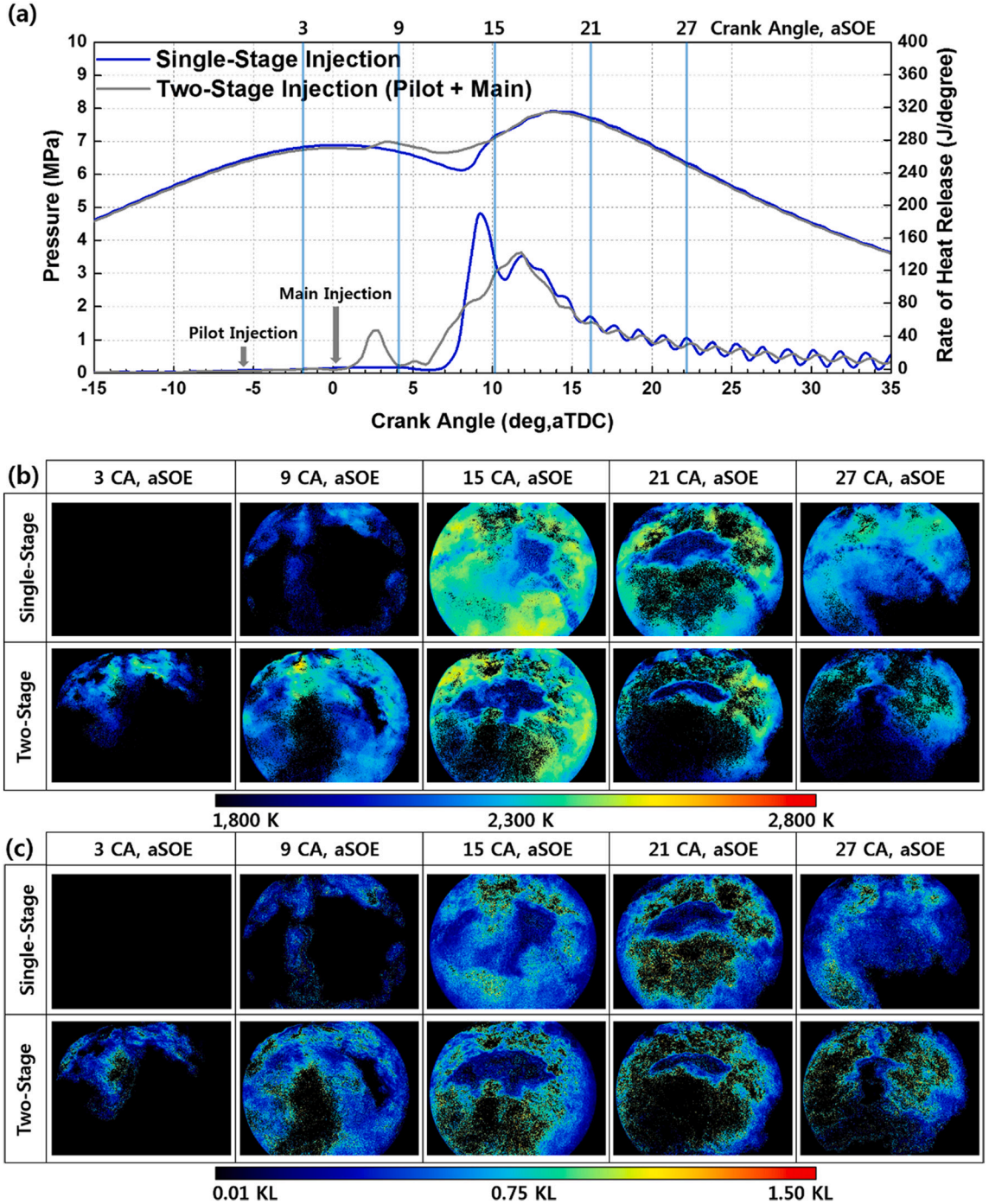

Fig. 7. (a) Cylinder pressure, (b) flame temperature, and (c) soot density data for the single and two-stage injections.

and pilot injection timing of aTDC –5.7°, which is the closest to the main injection timing, constitute the optimal pilot injection conditions. Although the PM emissions increased by applying the pilot injection, the optimum conditions were determined in consideration of the purpose of the pilot injection. Because the best anti-knocking performance was achieved under these pilot injection conditions. In addition to the metal engine experiments, optical engine experiments were performed with single and optimal pilot injection conditions to visually analyze the effect of the pilot injection on combustion temperature and soot density.

Fig. 7(a) compares the cylinder pressure and ROHR obtained under single-injection and two-stage injection conditions with respect to the CA. The two-stage injection is the same as the optimal pilot injection derived in the above experiments. Under single-injection conditions, a high intensity of premixed combustion occurred, followed by diffusion combustion. In contrast, the pilot injection promoted diffusion combustion by increasing the cylinder temperature. The flame temperature and soot density were derived by post-processing the combustion images obtained under the above experimental conditions. Figs. 7(b) and 7(c) show the images of the flame temperature and soot density for the single and two-stage injections, respectively. The post-processed figures indicate that the injection strategy affects the cylinder temperature and soot density. The images obtained at 3° and 9° CA, aSOE, reveal that the pilot injection reduces the ignition delay and promotes soot formation. The flame temperature and soot density remained low under single-injection conditions at the beginning of combustion. As premixed.

combustion occurred, the flame temperature and soot density rapidly increased. The differences between the single injection and two-stage injections could not be confirmed from the combustion images and cylinder pressure after 15° CA, aSOE. Moreover, a simple comparison of combustion images is not sufficient to identify the differences in combustion characteristics under different injection strategies. To overcome this limitation, this study obtained the values of the flame temperature and soot density from the combustion images. Fig. 8(a) shows the trends for the flame temperature and soot density for the single and two-stage injections. The hollow points indicate the average values of the flame temperature and soot density of all pixels in each combustion image. The solid points represent the average values of the hollow points for a specific CA. All points changed according to a certain trend from the start to the end of the observation period, which depended on the fuel injection strategies.

Based on the combustion images, the combustion period can be divided into two sections. During the first half of the combustion period, the flame temperature and soot density increased until the peak point, and this period was defined as the period of flame propagation and soot formation. Although soot formation and oxidization occurred simultaneously throughout the combustion period, soot formation was higher than soot oxidation during this period. The flame temperature and soot density steadily decreased until the end of the observation period. While NOx formation is closely related to the peak value of the flame temperature, the PM emissions are proportional to the soot density at the end of the observation period. The flame temperature and soot density were lower than those obtained under two-stage injection conditions at the start of the observation period because premixed combustion occurred under single-injection conditions. The premixed combustion by a single injection increased the peak flame temperature and simultaneously resulted in a low soot density. Conversely, the pilot injection inevitably increased the soot density, which was maintained until the end of the observation period. Fig. 8(b) summarizes the trends of the flame temperature and soot density for the single and two-stage injections. This figure shows the differences between premixed and diffusion combustion. As mentioned above, a low flame temperature and soot density were observed at the start of the observation period when a single injection was utilized. The single injection effectively increased not only the flame temperature but also the soot density. In contrast, the two-stage injection led to a high flame temperature and soot density at the start of the observation period, and it did not dramatically increase

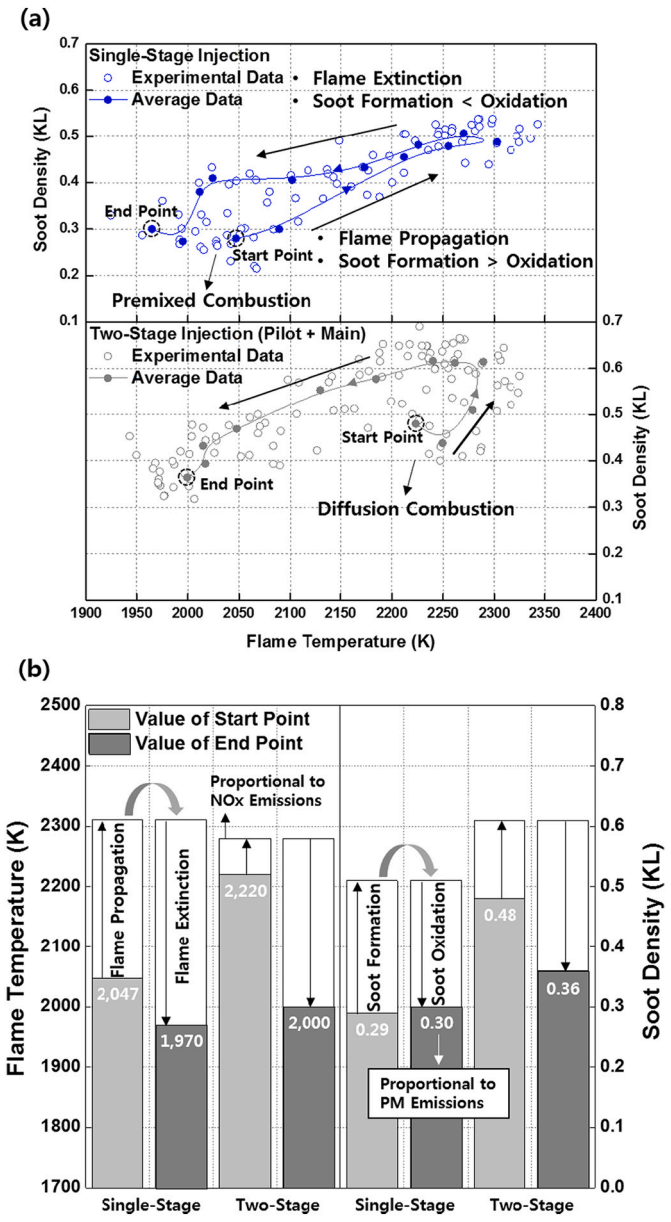

Fig. 8. (a) Experimental distributions and (b) trends for the flame temperature and soot density under single and two-stage injections.

both values during the first half of the observation period. In this period, the flame temperature and soot density increased by approximately 270 K and 0.22 KL, respectively, when a single injection was utilized. The two-stage injection increased the flame temperature and soot density by approximately 60 K and 0.13 KL, respectively. As a result, the peak flame temperature under two-stage injection conditions was lower than of the single-injection conditions, which can explain the NOx emission trends. The difference in soot density was reduced compared to the start of the observation, but the soot density was still higher in the two-stage injection.

The trends of flame extinction and soot formation under both experimental conditions were almost the same. This is because diffusion combustion commonly occurs regardless of the experimental conditions during the second half of the observation period. The injection strategy determined the flame temperature and soot density at the start of the observation period. Although almost the same soot oxidation rate was achieved under both conditions, the soot density at the end of the observation period was 0.07 KL higher under the two-stage injection

conditions than under the single-injection conditions, which was the same trend as for the PM emissions. The combustion image analysis revealed that the high PM emissions due to the pilot injection were attributed to the high soot density at the start of the observation period. In addition, the pilot injection prevented NOx formation by suppressing rapid combustion.

3.2. Post-injection experiments

The use of a pilot injection prevents rapid premixed combustion, which leads to knocking combustion and high NOx emissions. A post injection is mainly used to enhance the oxidization of incomplete combustion materials. In this part of the study, engine experiments were performed to analyze the effects of post-injection strategies on the combustion and emission characteristics. During the post-injection experiments, the optimal pilot injection conditions determined in previous experiments were applied.

3.2.1. Single-stage post-injection experiments

Before performing the engine experiments for multiple post injections, the effects of a single post injection on combustion and emission characteristics were determined. The single-stage post-injection timing was fixed at aTDC 9.2° because a better performance is achieved when the post-injection timing is close to the main injection timing. The post-injection quantity was varied from 3 to 9 mm^3/cycle with 3 mm^3/cycle intervals. The results of single-stage post injection were compared with those of a two-stage injection consisting of a pilot injection and a main injection without a post injection. Fig. 9 shows the cylinder pressure and ROHR with respect to the CA for various post-injection quantities, and noticeable differences can be observed between the results obtained with the different injection strategies. Because the total fuel injection quantity was fixed in all experiments, the main injection quantity was reduced by the post-injection quantity, resulting in low peak values of cylinder pressure and ROHR.

during the main combustion period. Fig. 10 shows the effect of the post-injection fuel quantity on the IMEPnet and thermal efficiency of the engine under single post-injection conditions. Because the post-injection timing was close to the main injection timing, the cylinder temperature was sufficiently high for combustion of the post-injected fuel. Under these conditions, a post injection promotes the oxidation of incomplete combustion materials. Furthermore, the lowered peak cylinder pressure achieved by applying a post injection reduced the heat loss, leading to high engine efficiency. As a result, the IMEPnet and thermal efficiency steadily improved by increasing the post-injection quantity within the error range. Although a post injection has a small effect on engine efficiency, the above results clearly reveal that it can improve engine efficiency under sufficiently high cylinder pressure conditions. The effects of a post injection on the oxidation of incomplete combustion materials are corroborated by the.

emission and lambda values provided in Fig. 11. Fig. 11 depicts the THC, CO, and PM emissions for various post-injection quantities. The emission results were normalized by those of the condition without a post injection. The post injection effectively reduced the incomplete combustion materials; however, an increase in PM emissions at a post-injection quantity of 3 mm^3/cycle was observed. In particular, the THC and CO emissions were greatly reduced after the injection. The THC and CO emissions were all lower than those achieved under conditions with no post injection. According to previous studies, THC is mainly generated in the crevice volume, where the cylinder temperature is relatively low [9]. In addition, CO formation occurs in the rich air-fuel mixture region because of the low O_2 concentration. Fig. 12 explains why post injection reduced the THC, CO, and PM emissions in the combustion chamber. At the end of the main injection, incomplete combustion occurs in locally high equivalence regions and in the crevice volume, which has a low combustion temperature. As a result, unburned combustion materials form. The post-injected fuel provided air to incomplete combustion materials in the combustion chamber or moved unburned gases in the low-temperature region to the high-temperature region for complete combustion, reducing THC, CO, and PM emissions. As the post-injection quantity increased, the CO and PM emissions were greatly reduced, but the THC oxidization effect was slightly reduced. This is because the post injection has the conflicting effects of reducing the peak cylinder pressure and moving the unburned material to the high-temperature region. In contrast, CO and PM formation is affected more by the local O_2 concentration than the cylinder temperature.

The lambda values demonstrate that increasing the post-injection quantity improves the thermal efficiency of the engine by reducing incomplete combustion materials. The lambda value is a representative indicator of complete combustion under the experimental conditions in which the total fuel injection quantity is fixed. In Fig. 11, the higher the post-injection quantity, the lower the observed lambda values, which implies that the THC, CO, and PM are oxidized more by post injection, resulting in high combustion efficiency. Complete combustion improves the IMEPnet and thermal efficiency of the engine, as shown in Fig. 10. The results of the experiments revealed that the pilot injection affects

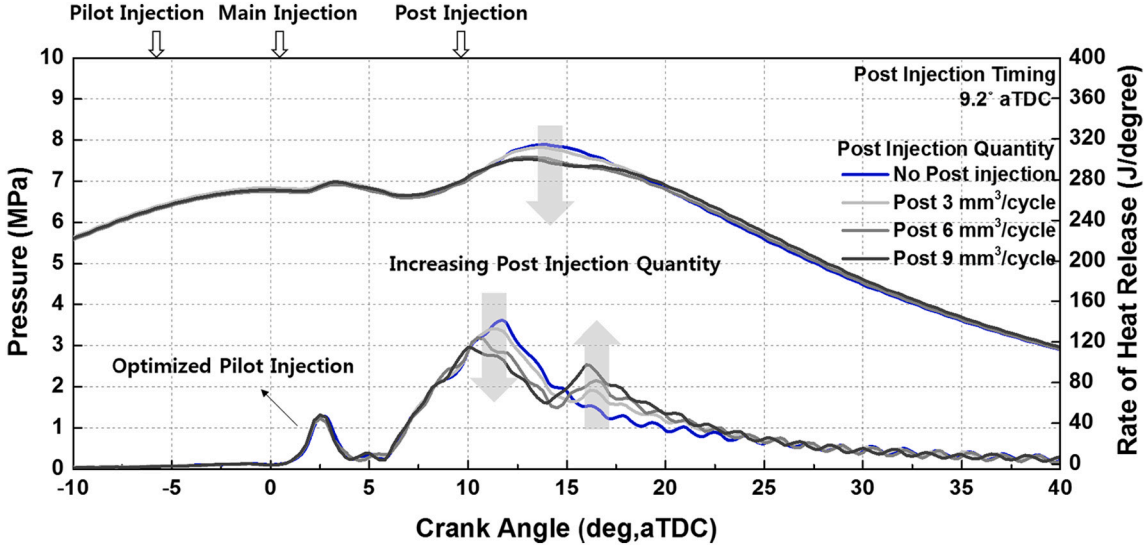

Fig. 9. Effects of a single-stage post injection on cylinder pressure and ROHR.

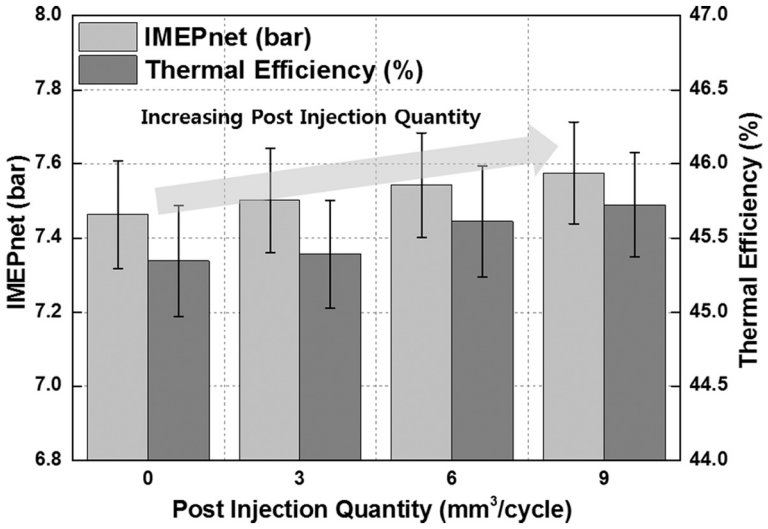

Fig. 10. Effects of a single-stage post injection on IMEPnet and thermal efficiency.

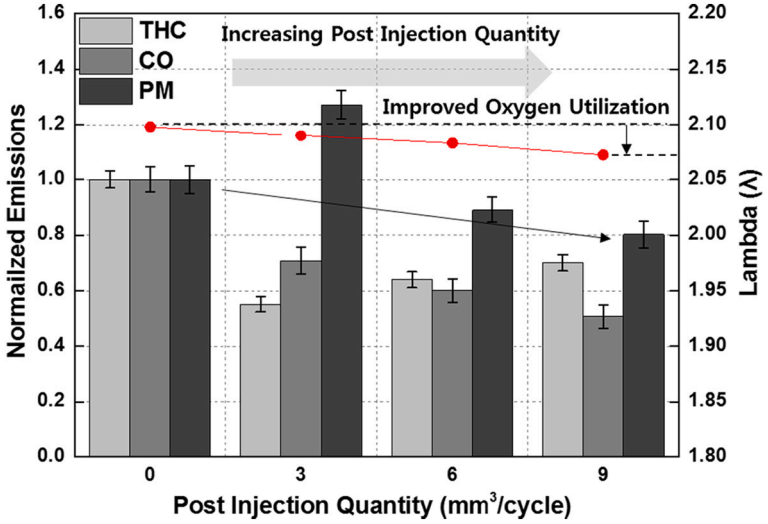

Fig. 11. Effects of a single-stage post injection on THC, CO, and PM emissions, and the lambda value.

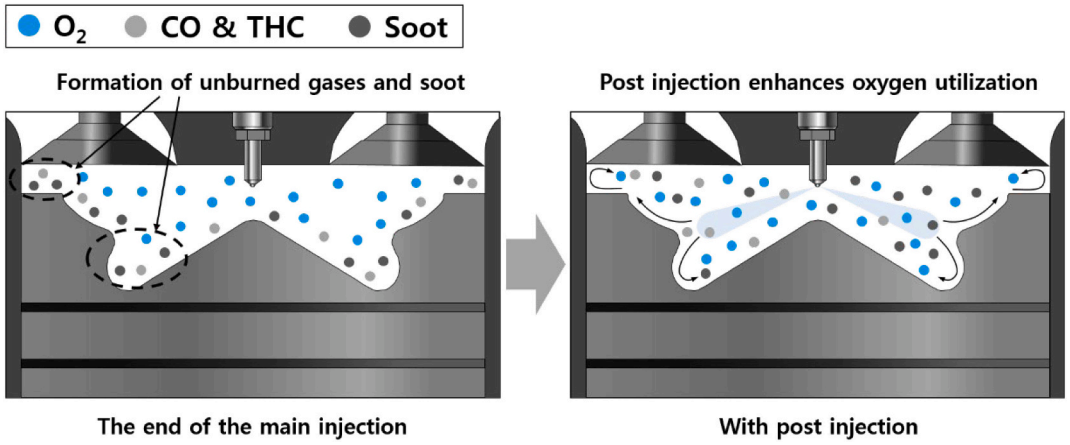

Fig. 12. Effects of a post injection in the combustion chamber.

the combustion phasing, whereas the post injection promotes the oxidation of unburned materials, affecting the engine efficiency. Considering the results of engine efficiency and emissions, a single-stage post-injection quantity of at least 6 mm^3/cycle was considered reasonable.

3.2.2. *Multiple-stage post-injection experiments*

Under multiple post injections, emission characteristics can be improved or impaired depending on the post injection number, even if the total post-injection quantity is the same. Therefore, after the single-stage post-injection experiments, multiple-stage post-injection experiments were carried out with different injection numbers and quantities. Fig. 13 shows the cylinder pressure and ROHR with respect to the CA under different multiple-stage post-injection conditions. As in the previous experiments, increasing the post-injection quantity reduced the peak cylinder pressure because of the lower main injection quantities. By analyzing the ROHR, it is possible to compare the number of post injections and post-injection quantities. The ROHR tended to increase gradually as the number of post injections increased, and cylinder pressure increased simultaneously. If incomplete combustion does not occur, the cylinder pressure at a particular CA is the same at the end of combustion with the same total injection quantity and driving condition, regardless of the number of injections. In other words, the cylinder pressure is lowered by the occurrence of incomplete combustion despite the same post-injection quantity conditions. The results for the second post-injection quantity of 3 mm^3/cycle, which resulted in a low cylinder pressure at the end of combustion, indicate incomplete combustion. Because the second post-injection timing is far from the TDC compared with the first post-injection timing, the cylinder temperature is insufficient for complete combustion of a small amount of post-injected fuel. In addition to the cylinder pressure, incomplete combustion affects the IMEPnet and thermal efficiency, as shown in.

Fig. 14 In this figure, the IMEPnet and thermal efficiency of the second post-injection quantity of 3 mm^3/cycle showed apparently lower values compared to other conditions that have the same post-injection quantity, and it is demonstrated that incomplete combustion deteriorates engine performance. In particular, the post-injection quantity of 6 + 3 mm^3/cycle led to the lowest IMEPnet and thermal efficiency, which exceeded the error range compared to other conditions. In contrast, the engine performance was improved by increasing the second post-injection quantity from 3 to 6 mm^3/cycle. Moreover, the third post-injection quantity of 6 mm^3/cycle was sufficient for combustion, as shown in Figs. 13 and 14. The emission and lambda values support the

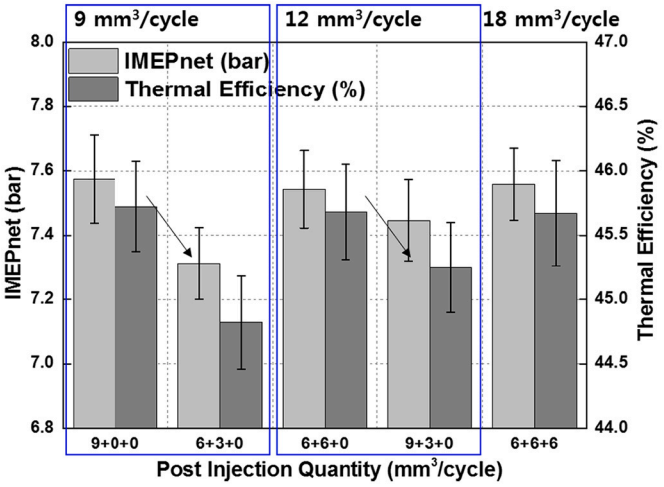

Fig. 14. Effects of multiple-stage post injection on IMEPnet and thermal efficiency.

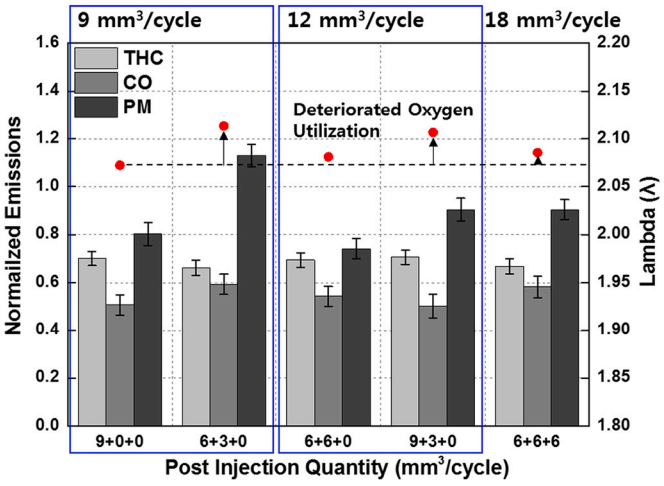

Fig. 15. Effects of multiple-stage post injection on THC, CO, and PM emissions, and the lambda value.

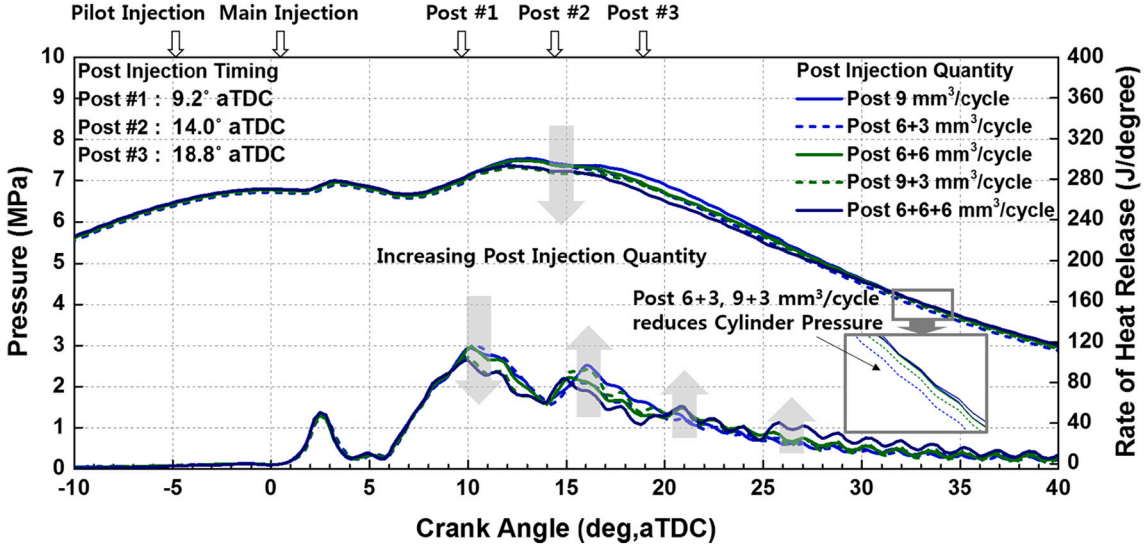

Fig. 13. Effects of multiple-stage post-injection strategies on cylinder pressure and ROHR.

above analysis based on the combustion characteristics. The effects of multiple-stage post-injection strategies on emissions and lambda values are shown in Fig. 15. In particular, high PM emissions and lambda values were mainly observed under conditions of deteriorated engine performance. It was revealed that the second post-injection quantity of 3 mm^3/cycle caused incomplete combustion, leading to high PM emissions and lambda values. In summary, the optimal post-injection condition was a two-stage post-injection of 6 + 6 mm^3/cycle, which not only maintained a relatively high thermal efficiency but also resulted in the most effective oxidation of incomplete combustion materials. Table 5 summarizes the optimal injection quantities and timings.

Figs. 16(a) and 16(b) show the effects of the pilot and post injections on the combustion and emission characteristics. The pilot injection prevented engine noise and vibration by reducing the premixed combustion ratio. However, an increase in PM emissions due to diffusion combustion is inevitable. By applying the post injection, it was confirmed that the increased PM emissions were reduced to the same level as the single-injection condition. Furthermore, the four-stage injection improved the thermal efficiency by reducing both heat loss and incomplete combustion materials. In conclusion, this study found that the application of the optimal multi-stage injection has obvious advantages in terms of combustion and emission characteristics. The effects of the post injection on the flame temperature and soot density are discussed next.

Fig. 17(a) shows the effects of post injection on the cylinder pressure and ROHR. Under both conditions, the same cylinder pressure and ROHR were obtained until the timing of 15° CA aSOE. The peak cylinder pressure and ROHR were reduced by applying a two-stage post injection. At timings of 21° and 27° CA aSOE, the ROHRs of the four-stage injection were higher than those of the other cases. In addition, the post injection led to a high cylinder pressure after the timing of 27° CA aSOE by enhancing the complete combustion. Figs. 17(b) and 17(c) show the flame temperatures and soot densities for the two-stage and four-stage injections, respectively. Under both conditions, the flame temperature and soot density were clearly observed from the beginning of the combustion period owing to the pilot injection. Almost the same flame temperature and soot density were maintained during the main combustion period. In addition to the cylinder pressure and ROHR, differences in the flame temperature and soot density obtained with the injection strategies were observed after 21° CA aSOE. The flame temperature of the four-stage injection was maintained after 21° CA aSOE, but it was not the highest flame temperature that resulted in significant NOx emissions. A high maintained flame temperature promoted soot oxidation. In addition, post injection increased the momentum energy in the combustion chamber, and a wide range of flame surfaces could be observed. As a result, the images of soot density showed opposite trends with the flame temperature at the end of the observation period.

For a more detailed analysis, Fig. 18(a) provides the trends of the flame temperature and soot density for the two-stage and four-stage injections. During the first half period, the two-stage injection increased the peak flame temperature, which was ascribed to high NOx emissions. The effects of the post injection on the flame temperature and soot density were mainly observed in the second half period. The results of the four-stage injection show a higher gradient of soot density versus flame temperature than that of the two-stage injection. This indicates that the soot density was rapidly reduced by the post injection, which enhanced soot oxidization. As a result, the soot density at the end of the observation showed a significant difference in accordance with the post-injection application.

Table 5
Conditions of the optimal multiple injections.

Order	Injection timing (deg, aTDC)	Injection Quantity (mm^3/cycle)
Pilot	–5.7	3
Main	0.13	36
Post 1	9.2	6
Post 2	14.0	6

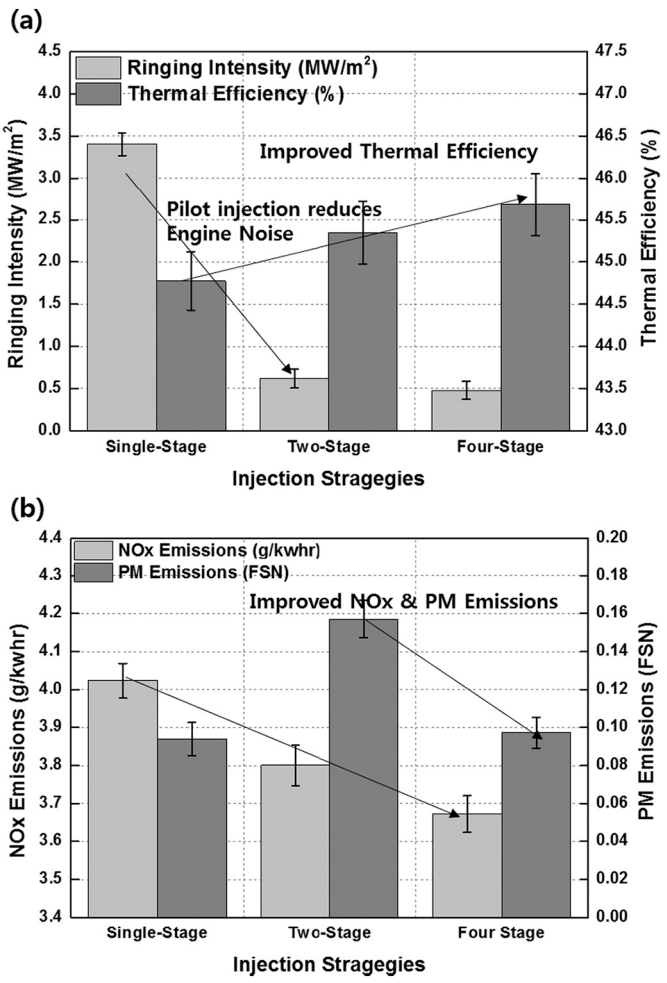

Fig. 16. Effects of multiple injection strategies on (a) combustion and (b) emission characteristics.

Fig. 18(b) summarizes the trends of the flame temperature and soot density obtained with the two-stage and four-stage injections. As mentioned above, the two-stage injection led to a high flame temperature of approximately 70 K compared with the four-stage injection. Both cases showed a peak soot density of approximately 0.61 KL. The post injection mainly affects soot oxidization during the second half of the period. In this period, the soot density reduced from 0.61 KL to 0.36 KL under two-stage injection conditions, and the four-stage injection reduced the soot density to approximately 0.32 KL, which was almost the same as the soot density at the end of the observation period when a single injection was utilized. The measured PM emissions under both injection strategies were also almost the same. Because the KL value calculated from the combustion images is a dimensionless value, it is difficult to simply compare the KL value and the measured PM emissions. Nevertheless, in this experiment, it was found that the KL value was sufficiently reliable by comparing the trends of the KL value at the end of the observation period and the measured PM emissions under the same conditions of combustion image acquisition.

4. Conclusions

The goals of this study were to optimize multiple-stage injections and conduct an optical analysis of the effects of multiple injections on the combustion process in a heavy-duty diesel engine. In addition to conventional analysis, the ringing intensity, which represents knocking

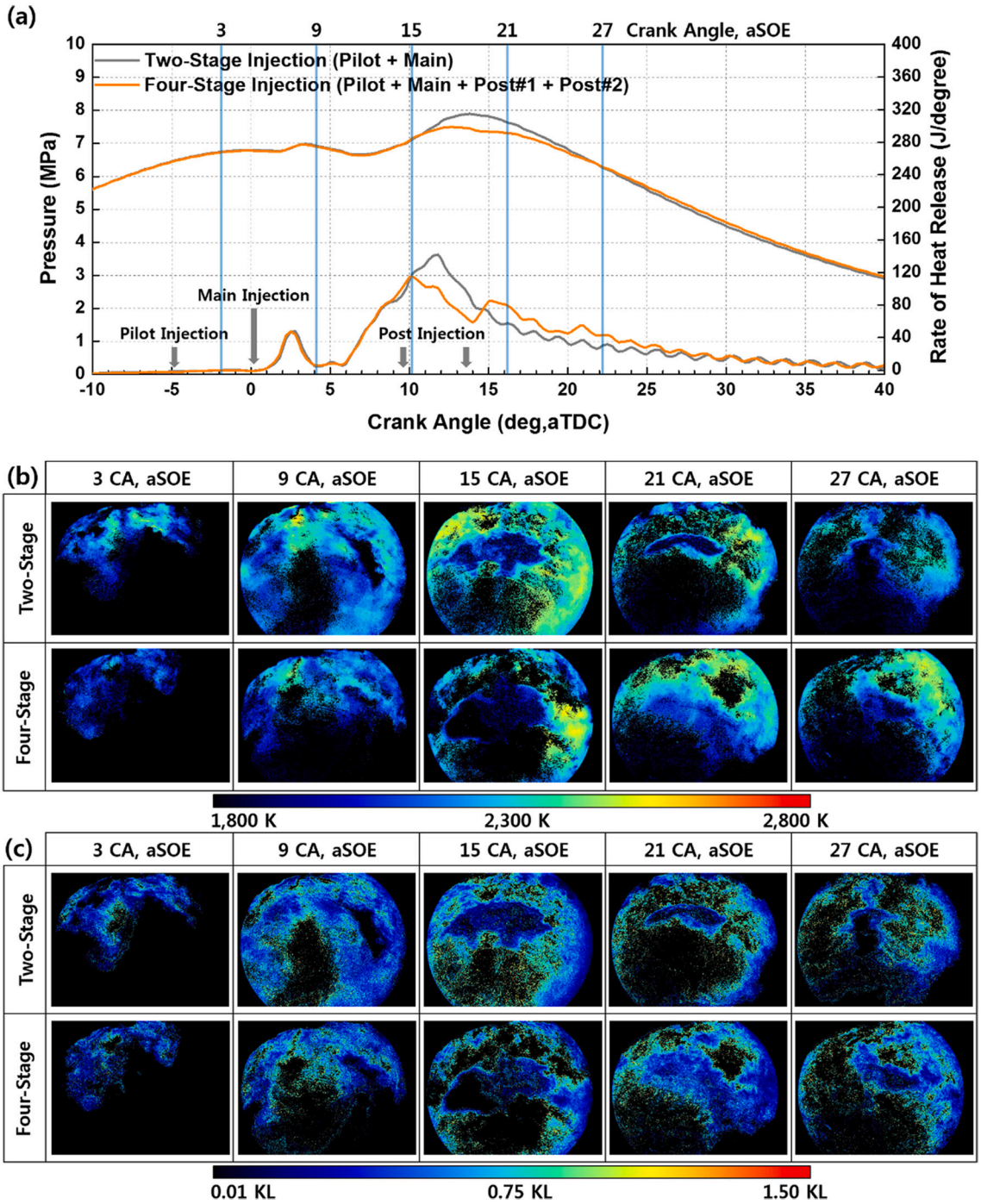

Fig. 17. (a) Cylinder pressure, (b) flame temperature, and (c) soot density data under two-stage and four-stage injection conditions.

combustion, was obtained to evaluate the engine noise and vibration. Optical engine experiments were performed using endoscopic visualization devices. The flame temperature and soot density were calculated from combustion images. The main conclusions of the engine experiments are summarized as follows:

1. The combustion of a single injection had a long ignition delay, which led to premixed combustion. As a result of the high intensity of premixed combustion, severe engine noise and vibration occurred. The long ignition delay results in a homogeneous air-fuel mixture, which effectively reduces PM emissions.
2. The main objective of the pilot injection is to prevent engine noise and vibration. The pilot-injected fuel was combusted, and the combustion chamber temperature increased. Therefore, the ignition delay was reduced, and moderate diffusion combustion occurred. The pilot injection timing and quantity affected the combustion and emission characteristics, respectively. While the IMEPnet and thermal efficiency were affected by the pilot injection timing, the pilot injection quantity determined the NOx and PM emissions. The optimized pilot injection strategy improved engine stability and thermal efficiency. However, increasing PM emissions were inevitable under pilot injection conditions because of diffusion combustion.
3. The post-injected fuel promoted the mixing of air and incomplete combustion materials in the combustion chamber, enhancing O_2 utilization. The THC, CO, and PM emissions were reduced by

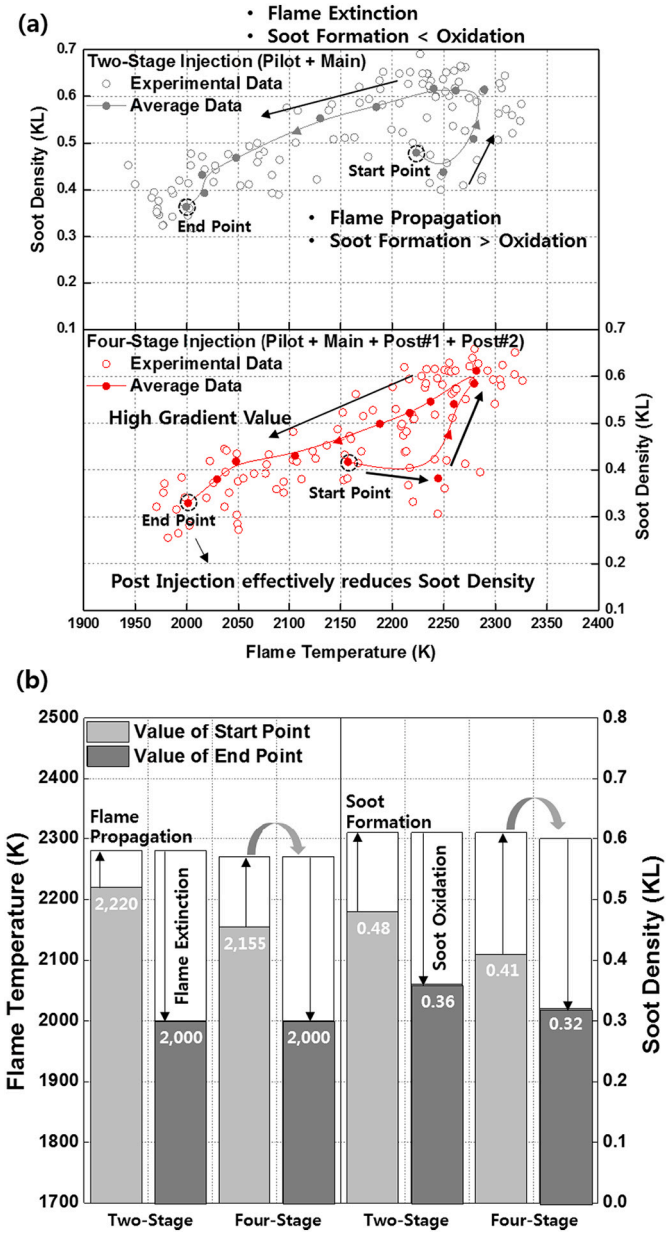

Fig. 18. (a) Experimental distributions and (b) trends of the flame temperature and soot density under two- and four-stage injections.

applying the post-injection strategy. Moreover, a lower peak cylinder pressure reduced heat loss, improving the IMEPnet and thermal efficiency. However, inappropriate post-injection conditions such as a too low injection quantity or retarded injection caused incomplete combustion, deteriorating the thermal efficiency and increasing the PM emissions.

4. Based on the combustion images, the combustion period can be divided into two sections. During the first half of the combustion period, flame propagation occurred, and the soot formation intensity was higher than the soot oxidation intensity, increasing the soot density. In contrast, the flame temperature and soot density decreased during the second half of the period. The peak flame temperature is closely related to the NOx emissions, and the PM emissions are proportional to the soot density at the end of the observation.
5. The effects of the pilot and post injections on the flame temperature and soot density were clearly identified by performing optical engine experiments. The high PM emissions due to the pilot injection were ascribed to the high soot density at the beginning of fuel combustion. The pilot injection reduced the peak flame temperature by suppressing the high-intensity premixed combustion. The post injection lowered the peak flame temperature and enhanced soot oxidation, resulting in low NOx and PM emissions.

5. Future work

In this study, a tungsten lamp was used to calibrate the apparent temperature. Moreover, the CCD camera used in this study was relatively small and had a low resolution. These elements cause errors in combustion image analysis. To overcome these errors, a black body and an improved combustion image acquisition system that contains a spectrograph and high-resolution CCD camera will be used in future research.

Author's contributions

Minhoo Choi and Sungwook Park designed the experiments. Minhoo Choi conducted the experiments, analyzed the results, and wrote the manuscript.

Declaration of Competing Interest

The authors declare that they have no known competing financial interests or personal relationships that could have appeared to influence the work reported in this paper.

Acknowledgments

This work was supported by the BK21 FOUR (Fostering Outstanding Universities for Research) program through the National Research Foundation (NRF) funded by the Ministry of Education of Korea.

References

[1] J.L. Sullivan, R.E. Baker, B.A. Boyer, R.H. Hammerle, T.E. Kenney, L. Muniz, T. J. Wallington, CO2 Emission Benefit of Diesel (versus gasoline) Powered Vehicles, Environ. Sci. Technol. 38 (2004) 3217–3223.
[2] B. Dhinesh, J. Isaac Joshua Ramesh Lalvani, M. Parthasarathy, K. Annamalai, An assessment on performance, emission and combustion characteristics of single cylinder diesel engine powered by Cymbopogon flexuosus biofuel, Energy Convers. Manag. 117 (2016) 466–474.
[3] S. Kimura, O. Aoki, Y. Kitahara, E. Aiyoshizawa, Ultra-Clean Combustion Technology Combining a Low-Temperature and Premixed Combustion Concept for Meeting Future Emission Standards, SAE International, 2001.
[4] J.H. Jeong, D.W. Jung, O.T. Lim, Y.D. Pyo, Y.J. Lee, Influence of pilot injection on combustion characteristics and emissions in a DI diesel engine fueled with diesel and DME, Int. J. Automot. Technol. 15 (2014) 861–869.
[5] B.M.V. Twigg, P.R. Phillips, Cleaning the air we breathe-controlling diesel particulate emissions from passenger cars, Platin. Met. Rev. 53 (2009) 27–34.
[6] R. Hauser, E.A. Eisen, L. Pothier, D.C. Christiani, A prospective study of lung function among boilermaker construction workers exposed to combustion particulates, Am. J. Ind. Med. 39 (2001) 454–462.
[7] M. Williams, R. Minjares, A Technical Summary of Euro 6/VI Vehicle Emission Standards, International Council for Clean Transportation (ICCT), Washington, DC, 2017. Accessed July, 10 (2016).
[8] G.K. Lilik, A.L. Boehman, Advanced diesel combustion of a high cetane number fuel with low hydrocarbon and carbon monoxide emissions, Energy Fuel 25 (2011) 1444–1456.
[9] S. Imtenan, M. Varman, H.H. Masjuki, M.A. Kalam, H. Sajjad, M.I. Arbab, I.M., Rizwanul Fattah, Impact of low temperature combustion attaining strategies on diesel engine emissions for diesel and biodiesels: a review, Energy Convers. Manag. 80 (2014) 329–356.
[10] M. Alriksson, I. Denbratt, Low Temperature Combustion in a Heavy Duty Diesel Engine Using High Levels of EGR, SAE International, 2006.
[11] R. Kiplimo, E. Tomita, N. Kawahara, S. Yokobe, Combustion and Emission Characteristics of a Premixed Charge Compression Ignition Engine, 2016.
[12] S.H. Min, H.K. Suh, J. Cha, Effect of Simulated-EGR (N2) on the distribution characteristics of equivalence ratio and the formation of exhaust emissions in a CI engine under early injection conditions, Energy 193 (2020), 116850.
[13] S. Singh Kalsi, K.A. Subramanian, Experimental investigations of effects of EGR on performance and emissions characteristics of CNG fueled reactivity controlled compression ignition (RCCI) engine, Energy Convers. Manag. 130 (2016) 91–105.

[14] F. Zhang, H. Xu, S. Zeraati Rezaei, G. Kalghatgi, S.-J. Shuai, Combustion and Emission Characteristics of a PPCI Engine Fuelled with Dieseline, SAE International, 2012.
[15] W. Kang, B. Choi, S. Jung, S. Park, PM and NOx reduction characteristics of LNT/DPF+SCR/DPF hybrid system, Energy 143 (2018) 439–447.
[16] E. Mancaruso, S.S. Merola, B.M. Vaglieco, Study of the multi-injection combustion process in a transparent direct injection common rail diesel engine by means of optical techniques, Int. J. Eng. Res. 9 (2008) 483–498.
[17] T. Tanaka, A. Ando, K. Ishizaka, Study on pilot injection of DI diesel engine using common-rail injection system, JSAE Rev. 23 (2002) 297–302.
[18] T. Sato, M. Yamada, K. Michio, T. Fujimura, K. Nagata, Development of a Mechanical Pilot Injection Device for Automotive Diesel Engines, SAE International, 1989.
[19] L. Zhang, A Study of Pilot Injection in a DI Diesel Engine, SAE International, 1999.
[20] K.P. Mayer, Fuel Economy, Emissions and Noise of Multi-Spray Light Duty DI Diesels–Current Status and Development Trends, SAE International, 1984.
[21] S. Kook, C. Bae, P.C. Miles, D. Choi, L.M. Pickett, The Influence of Charge Dilution and Injection Timing on Low-Temperature Diesel Combustion and Emissions, SAE International, 2005.
[22] R.W. Hil, C.S. Lawrence, D.P. Clarke, J.R. Needham, The Optimized Direct Injection Diesel Engine for Future Passenger Cars, SAE International, 1988.
[23] T. Minami, K. Takeuchi, N. Shimazaki, Reduction of Diesel Engine NOx Using Pilot Injection, SAE International, 1995.
[24] M. Tsukahara, T. Chikahisa, N. Miyamoto, T. Murayama, A Study on the reduction of NOx of diesel engine by the use of an auxiliary injection method, Bull. JSME 24 (1981) 571–577.
[25] M. Badami, F. Millo, D.D. D'Amato, Experimental Investigation on Soot and NOx Formation in a DI Common Rail Diesel Engine with Pilot Injection, SAE International, 2001.
[26] M. Ishida, Z.-L. Chen, G.-F. Luo, H. Ueki, The Effect of Pilot Injection on Combustion in a Turbocharged D. I. Diesel Engine, SAE International, 1994.
[27] H. Ishiwata, T. Ohishi, K. Ryuzaki, K. Unoki, N. Kitahara, A Feasibility Study of Pilot Injection in TICS (timing and Injection Rate Control System), SAE International, 1994.
[28] T. Shimada, T. Shoji, Y. Takeda, The Effect of Fuel injection Pressure on Diesel Engine Performance, SAE International, 1989.
[29] S. Shundoh, M. Komori, K. Tsujimura, S. Kobayashi, NOx Reduction from Diesel Combustion Using Pilot Injection with High Pressure Fuel Injection, SAE International, 1992.
[30] Y. Hotta, M. Inayoshi, K. Nakakita, K. Fujiwara, I. Sakata, Achieving Lower Exhaust Emissions and Better Performance in an HSDI Diesel Engine with Multiple Injection, SAE International, 2005.
[31] J. Benajes, S. Molina, J.M. García, Influence of Pre- and Post-Injection on the Performance and Pollutant Emissions in a HD Diesel Engine, SAE International, 2001.
[32] S.K. Chen, Simultaneous Reduction of NOx and Particulate Emissions by Using Multiple Injections in a Small Diesel Engine, SAE International, 2000.
[33] S. Nimodia, K. Senthilkumar, V. Halbe, P.R. Ghodke, R. Velusamy, Simultaneous Reduction of NOx and Soot Using Early Post Injection, The Automotive Research Association of India, 2013.
[34] S.M. Farhan, W. Pan, W. Yan, Y. Jing, L. Lili, Impact of post-injection strategies on combustion and unregulated emissions during different loads in an HSDI diesel engine, Fuel 267 (2020), 117256.
[35] M. Badami, F. Mallamo, F. Millo, E.E. Rossi, Experimental investigation on the effect of multiple injection strategies on emissions, noise and brake specific fuel consumption of an automotive direct injection common-rail diesel engine, Int. J. Eng. Res. 4 (2003) 299–314.
[36] A. Sperl, The Influence of Post-Injection strategies on the Emissions of Soot and Particulate Matter in Heavy Duty Euro V Diesel Engine, SAE International, 2011.
[37] W.L. Hardy, R.D. Reitz, An Experimental Investigation of Partially Premixed Combustion Strategies Using Multiple Injections in a Heavy-Duty Diesel Engine, SAE International, 2006.
[38] D.A. Pierpont, D.T. Montgomery, R.D. Reitz, Reducing Particulate and NOx using Multiple Injections and EGR in a D.I. Diesel, SAE International, 1995.
[39] Y. Tominaga, H. Tajima, A. Strom, K. Uno, Flame temperature measurement in diesel engine on two color method utilizing CMOS Camera(Measurement, Temperature), Proceed. Int. Symp. Diagnost. Model. Combust. Int Comb. Eng. 2004 (6) (2004) 7–12.
[40] X. Cheng, L. Chen, F. Yan, G. Hong, Y. Yin, H. Liu, Investigations of Split Injection Strategies for the Improvement of Combustion and Soot Emissions Characteristics Based On the Two-Color Method in a Heavy-Duty Diesel Engine, SAE International, 2013.
[41] S. Iorio, A. Magno, E. Mancaruso, B. Vaglieco, Diesel/methane dual fuel strategy to improve environmental performance of energy power systems, Int. J. Heat Technol. 34 (2016) S581–S588.
[42] M. Sjöberg, J.E. Dec, Effects of Engine Speed, Fueling Rate, and Combustion Phasing on the thermal Stratification Required to Limit HCCI Knocking Intensity, SAE International, 2005.
[43] J.A. Eng, Characterization of Pressure Waves in HCCI Combustion, SAE International, 2002.
[44] K. Zha, R.-C. Florea, M. Jansons, Comparison of Soot Evolution Using High-Speed CMOS Color Camera and Two-Color Thermometry in an Optical Diesel Engine Fueled With B20 Biodiesel Blend and Ultra-Low Sulfur Diesel, 2011, pp. 273–294.
[45] Y. Matsui, T. Kamimoto, S. Matsuoka, A Study on the Application of the Two–Color Method to the Measurement of Flame Temperature and Soot Concentration in Diesel Engines, SAE International, 1980.
[46] Q. Shi, T. Li, X. Zhang, B. Wang, M. Zheng, Measurement of Temperature and Soot (KL) Distributions in Spray Flames of Diesel-Butanol Blends by Two-Color Method Using High-Speed RGB Video Camera, SAE International, 2016.